JACS
JOURNAL OF THE AMERICAN CHEMICAL SOCIETY
Article
pubs.acs.org/JACS

Sensing of Carboxylate Drugs in Urine by a Supramolecular Sensor Array

Yuanli Liu,[†] Tsuyoshi Minami,[†] Ryuhei Nishiyabu,[‡] Zhuo Wang,[†] and Pavel Anzenbacher, Jr.[†,*]

[†]Department of Chemistry and Center for Photochemical Sciences, Bowling Green State University, Bowling Green, Ohio 43403, United States

[‡]Department of Applied Chemistry, Graduate School of Urban Environmental Sciences, Tokyo Metropolitan University, Tokyo 192-0397, Japan

Supporting Information

ABSTRACT: A supramolecular sensor array consisting of eight chemosensors embedded in a hydrogel matrix was used to sense carboxylate drugs. The discriminatory power of the array has been evaluated using principal component analysis and linear discriminant analysis. The eight-member sensor array has been shown to accurately identify 14 carboxylates in water with 100% classification accuracy. To demonstrate the potential for practical utility in the physiological environment, analysis of carboxylate drugs in human urine was also performed achieving 100% correct classification. In addition, the array performance in semiquantitative identification of nonsteroidal anti-inflammatory drugs has been investigated, and the results show that the sensor array is able to differentiate six typical nonsteroidal anti-inflammatory drugs at concentrations of 0.5−100 ppm. This illustrates the potential utility of the designed sensor array for diagnostic and environmental monitoring applications.

INTRODUCTION

Carboxylates are important anions frequently encountered in Nature as well as in a number of biological processes. Their utility in the chemical, pharmaceutical, food, and beverage industry is widespread.[1] A number of drugs contain carboxylate function —notably nonsteroidal anti-inflammatory drugs (NSAIDs).[2] Due to their extensive use, these drugs also present a significant environmental burden.[3] For this study, we selected a group of carboxylates including antimalarial artesunate,[4] and well-known NSAIDs (ibuprofen, naproxen, diclofenac, flurbiprofen, ketoprofen, mefenamic acid) commonly used to relieve pain, inflammation, and fever.[2] Also included were aminoacids (alanine, tyrosine, sarcosine) and small-molecule carboxylates (mevalonate, thyroxine) known to play an important role in human metabolism. This is because sarcosine is a potential biomarker for human prostate cancer,[5] while mevalonic acid is an intermediate in steroid biosynthesis.[6] Tyrosine[7] is a precursor of catecholamine neurotransmitters and hormone thyroxine.

Current detection methods for carboxylates generally utilize solid-phase extraction (SPE) preconcentration while the analysis of the concentrated sample is typically performed by liquid chromatography−mass spectrometry,[8] or gas chromatography−mass spectrometry.[9] These methods, however, are not easily amenable to determination of carboxylates in biological fluids.

Recently, chemosensors possessing binding sites for carboxylates have been investigated[10] including sensors based on cross-reactive arrays inspired by the mammalian olfactory system.[11] The increased popularity of array-based sensors is largely due to their capability to recognize a number of analytes with high classification accuracy.[12] However, few sensor arrays exists for carboxylate anions that function in aqueous solution.[13] To the best of our knowledge, sensor arrays capable of sensing carboxylate anions in a complex biological milieu, such as human urine, have not yet been developed.

Previously, we demonstrated that calixpyrrole sensors doped into polyurethane films could be used for sensing of aqueous carboxylates. The preliminary experiments showed colorimetric sensing of three carboxylates of medical interest.[14] Inspired by this work, we developed a fluorescence-based sensor array capable of differentiation of fourteen pharmaceutically and biologically important carboxylates (Figure 1, top) in both water and urine with high classification accuracy. The array is prepared by casting a solution of polyurethane (**PU**) and octamethylcalix[4]pyrrole sensor (Figure 1, bottom) into a multiwell microtiter plate.

Additionally, this new chemosensor design utilizes both colorimetric and fluorimetric responses, which yields information-rich output useful for discrimination of analytes. The utility of this dual signal transduction scheme is demonstrated in semiquantitative identification of NSAIDs over a wide range of concentration.

RESULTS AND DISCUSSION

The sensors **S1**−**S7** utilize the octamethylcalix[4]pyrrole (OMCP)[15] receptor for anions including carboxylates, which

Received: February 12, 2013
Published: April 23, 2013

   dx.doi.org/10.1021/ja4015748 | J. Am. Chem. Soc. 2013, 135, 7705−7712

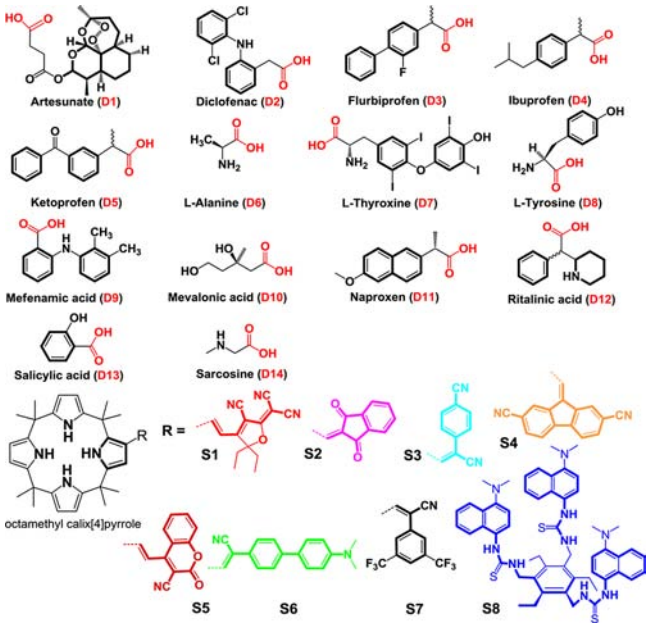

Figure 1. Molecular structures of target carboxylates **D1**–**D14** (top) and **S1**–**S8** used for the sensor array (bottom).

is an excellent structural platform for preparation of anion sensors. The information-rich signal output generated by **S1**–**S7** arises from attaching different chromophores to OMCP. One of the OMCP pyrroles communicates with an electron-withdrawing residue attached through a vinyl bridge.

This structural arrangement establishes an intramolecular partial charge transfer (IPCT) cascade (Figure 2): As the anion

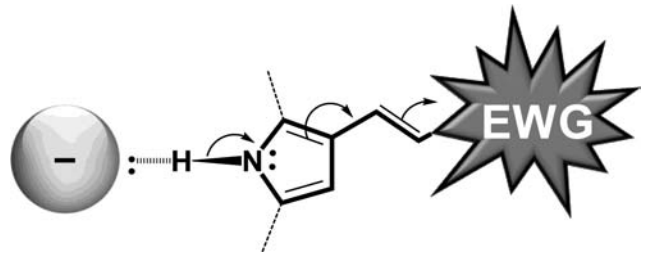

Figure 2. Intramolecular partial charge transfer (IPCT) in the sensors **S1**–**S7** results in anion-induced changes in fluorescence and color.

attracts the proton involved in hydrogen bonding, the electronic density of the H–N bond shifts toward the pyrrole nitrogen and causes further polarization of the pyrrole electronic cloud. An acceptor (electron-withdrawing moiety, EWG) attached through a conjugated bridge accommodates the excess partial charge, thus completing the partial charge transfer (IPCT) cascade.[10d,f,15b] The IPCT results in anion binding-induced changes in fluorescence or color.[15b,c,16] Sensor **S8**, a tripodal *turn-on* fluorescent sensor prepared from (2,4,6-triethyl-1,3,5-trimethylamino)benzene,[12e] shows selectivity for aliphatic carboxylates and phosphates (Table 1), and was included in the array to increase its signal variability. The sensor **S8** is flexible in the resting state but forms a stable bowl-shape complex with the anions. The increased rigidity of the complex results in limited nonradiative dissipation of the excited state energy, thereby increasing the fluorescence (turn-on signal). This, together with IPCT effect, results in an information-rich output by **S8**. Also, **S8**-anion complexes are likely to display C_3 symmetry, which is more complementary to phosphate anion. As a result, **S8** displays preference for phosphate.

The binding affinities of **S1**–**S8** for anions are shown in Table 1, which shows relatively high binding affinities of **S1**–**S7** toward halide and acetate anions over benzoate. The selection of the test group of anions was made using anions known to be bound by calix[4]pyrrole receptors.[15,17] **S8**, which does not show a significant response to halides, was expected to be an important factor in the analyte recognition by the array. This hypothesis was confirmed by the analysis of the contribution of the individual sensors.

To visualize the fingerprint-like response pattern of the **S1**–**S8** array to individual analytes, we show an image corresponding to a preliminary experiment comprising fluorescence recorded using three channels (blue, green, and red). Even with the naked eye, one can see that the addition of aqueous solutions of carboxylates (**D1**–**D14**) resulted in a fingerprint-like fluorescence response pattern (Figure 3). As

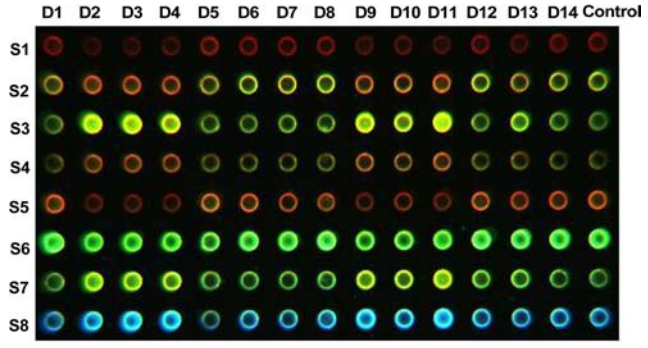

Figure 3. Fluorescence responses of the **S1**–**S8** sensor array to the presence of carboxylates **D1**–**D14** (1 mM in water at pH 8.5, 200 nL). The color representation was generated by superimposing equally weighted images corresponding to RGB channels.

Table 1. Binding Constants (M^{-1}) Derived from Titrations Using Sensors S1–S8 and Anions[a]

	sensors							
anions	**S1**	**S2**	**S3**	**S4**	**S5**	**S6**	**S7**	**S8**
F^-	$>1.0 \times 10^8$	2.1×10^6	2.5×10^6	1.0×10^7	1.0×10^7	1.6×10^6	1.6×10^5	ND
Cl^-	3.5×10^5	1.0×10^5	1.2×10^5	2.9×10^5	2.9×10^5	1.1×10^5	1.8×10^4	ND
AcO^-	2.6×10^6	4.2×10^5	4.1×10^5	5.8×10^5	1.1×10^6	2.8×10^5	9.9×10^4	1.6×10^4
$H_2PO_4^-$	2.1×10^6	6.5×10^4	8.1×10^4	5.8×10^4	6.2×10^4	4.1×10^4	3.6×10^4	4.3×10^5
$HPPi^{3-}$	ND	3.0×10^5	ND	4.8×10^5	ND	2.5×10^5	5.4×10^4	9.8×10^4
BzO^-	3.0×10^5	1.4×10^5	1.4×10^5	3.1×10^5	4.4×10^5	1.0×10^5	1.8×10^5	ND

[a]Binding constants were determined in MeCN (**S1**–**S7**) and DMSO (**S8**), respectively using anions in the form of their tetra-*n*-butylammonium salts. ND means not determined due to low affinity or biphasic nature of the isotherm. All errors are <15%.

dx.doi.org/10.1021/ja4015748 | *J. Am. Chem. Soc.* 2013, 135, 7705–7712

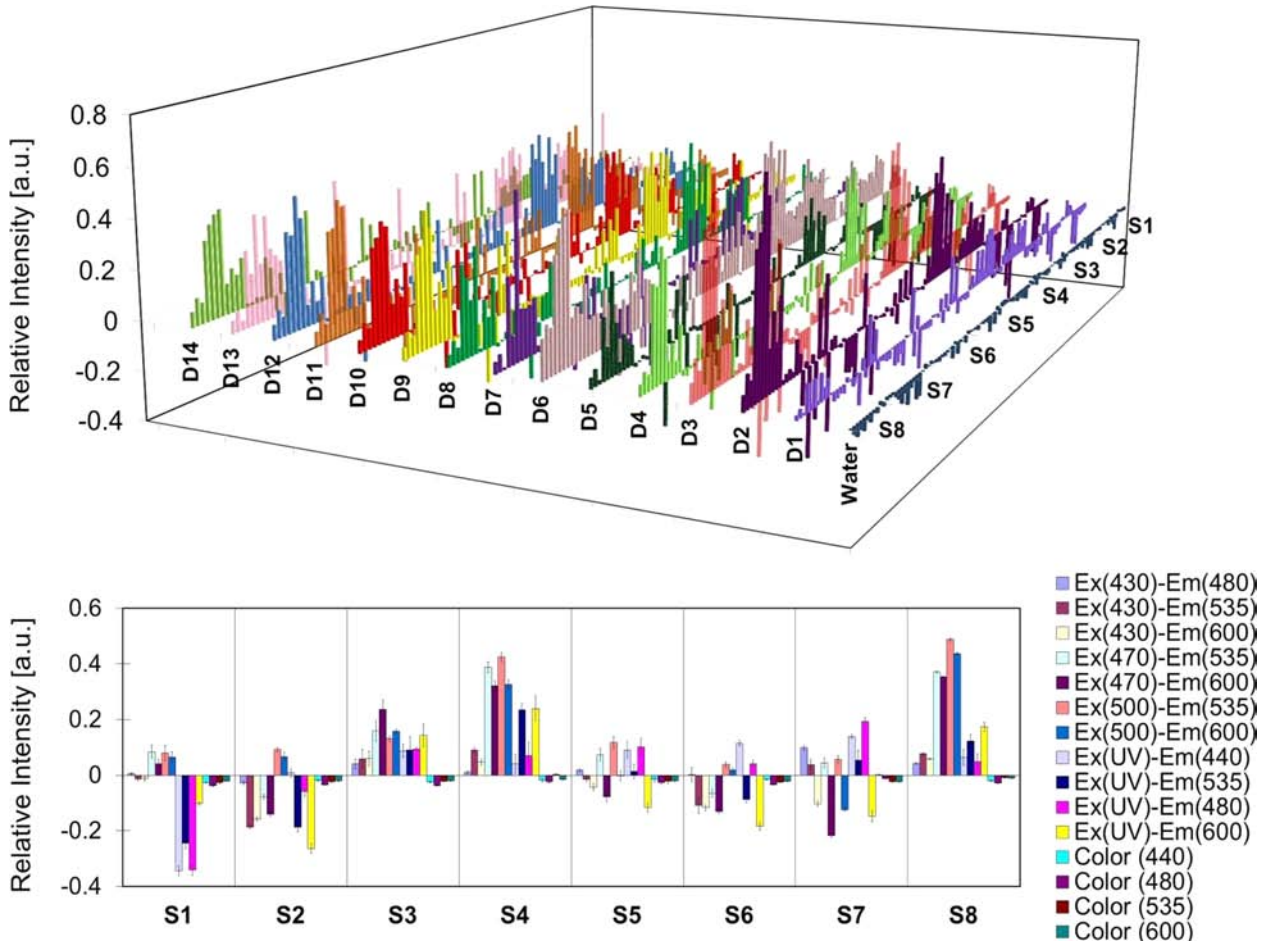

Figure 4. (Top) Pattern generated by **S1−S8** sensors array using 15 fluorescence and colorimetric channels in response to carboxylates **D1−D14** in water (500 μM, 200 nL, pH 8.5). (Bottom) Response profile of the **S1−S8** sensor array upon addition of ibuprofen, **D4**, (500 μM, 200 nL, pH 8.5).

expected, each sensor in the array generated a distinct change in the fluorescence imparted by the different carboxylates. This response pattern can be analyzed using methods of pattern recognition to achieve analytes discrimination.

Encouraged by the apparent information-rich response pattern, we attempted to discriminate the fourteen carboxylates (**D1**-**D14**) in aqueous solutions by the **S1−S8** sensor array. We have recorded the information from both the fluorimetric (eleven channels) and colorimetric (four channels) images. Figure 4 (top panel) shows the overall response pattern of the sensor array in the presence of carboxylates. As hypothesized, each carboxylate induced a distinctive change in the individual sensor. Figure 4 (bottom) shows a response of sensors **S1−S8** to ibuprofen (**D4**) with characteristic signal increases and decreases (relative to the control). This illustrates the assertion that a multidimensional response pattern matrix is created by compiling the (**D1−D14**) × (**S1−S8**) response data, which are then utilized in a pattern-recognition investigation.

The sensor array consisting of eight sensors generates a signal output in the form of a multidimensional response (120 dimensions = 15 channels × 8 sensors). The signal output comprises both fluorimetric and colorimetric data.[18] The array response was evaluated by utilizing the statistical multivariate analysis method - principal component analysis (PCA).[19] Here, the PCA of the data set (10 repetitions for each carboxylate) acquired from the eight-member sensor array requires 15 dimensions (PCs) out of 120 to describe 95% of the discriminatory range (12% of all PCs). This attests to an extraordinarily high degree of dispersion of the data obtained by the **S1−S8** sensor array. This discrimination capacity is unusually high in comparison with that reported for a sensor array generally displaying 95% of discrimination in the first two PCs.[11a,c] Here, the PCA score plot (Figure 5) shows clear

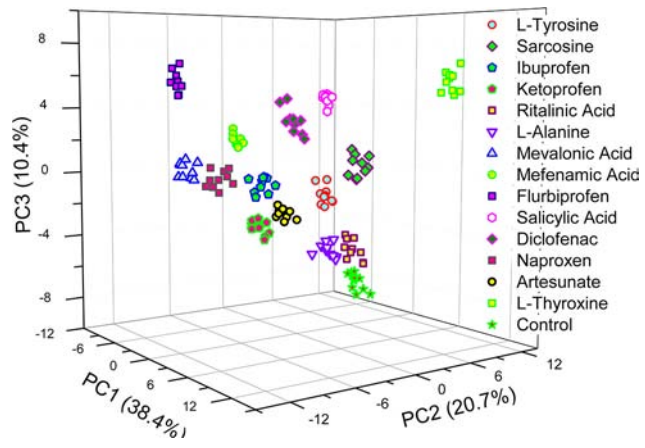

Figure 5. PCA score plot of the first three principal components of statistical significance for 150 samples (200 nL, 500 μM in water, pH 8.5, 14 carboxylates plus a control, 10 trials each) produced by the **S1−S8** sensors array.

dx.doi.org/10.1021/ja4015748 | J. Am. Chem. Soc. 2013, 135, 7705−7712

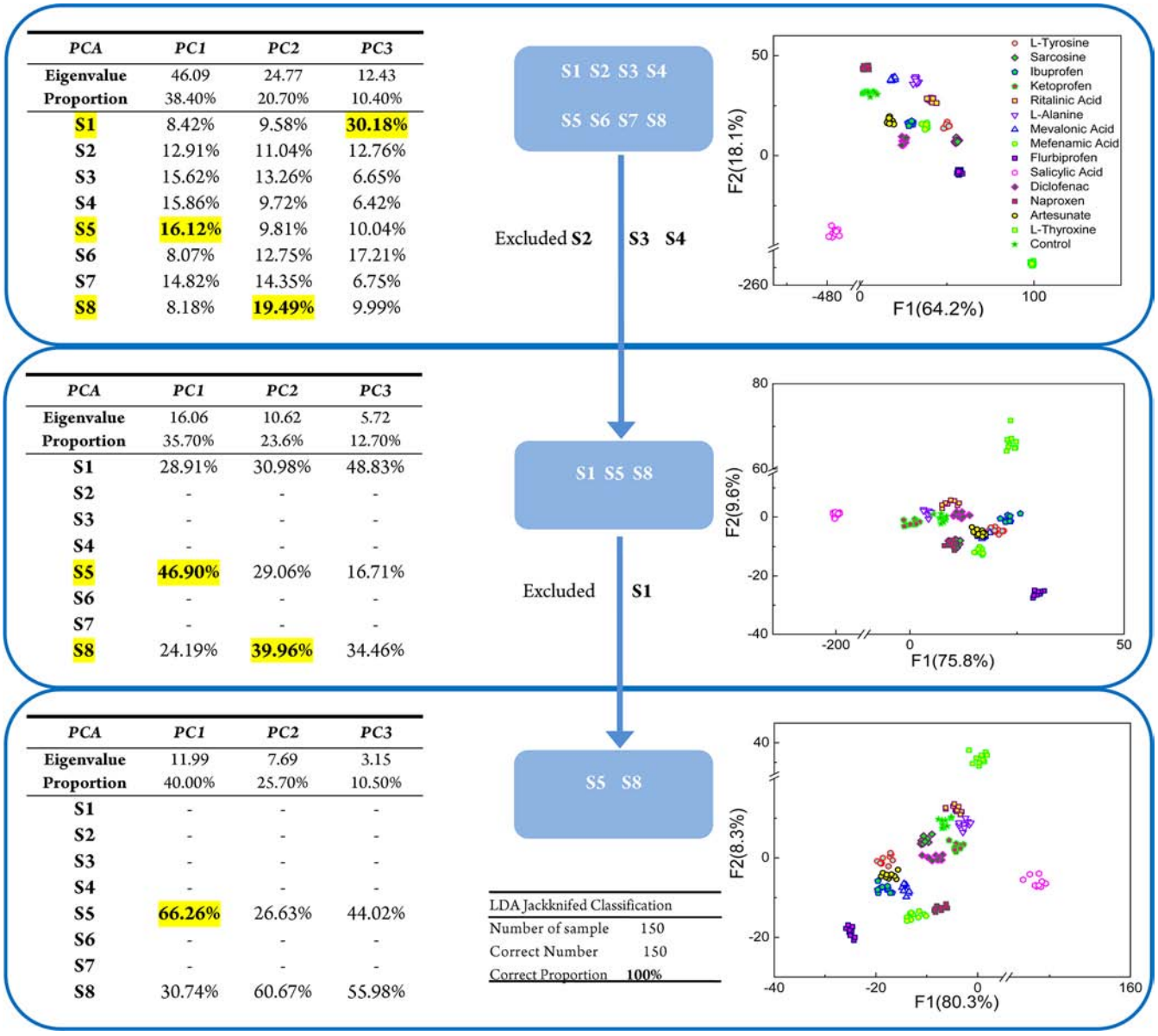

Figure 6. Schematic representation of the investigation of the most important contributors to the overall statistical significance: (Top) PCA for the complete set of sensors (**S1**–**S8**) shows that the main contributors to the cluster dispersion are **S1**, **S5**, and **S8**. (Center) Sensors **S2**, **S3**, **S4**, **S6**, and **S7** were excluded from the data set and the remaining data were analyzed again with PCA. PCA shows that the main contributors were **S5** and **S8**. (Bottom) **S1** was excluded and LDA was carried out using the remaining data set. Cross-validated LDA shows 100% accurate classification for all three arrays.

clustering of the data using only the first three PCs (representing 69.4% of variance). The high dispersion level of the data shown by the PCA score plot can be attributed to the differences in response of the IPCT-based sensors to the carboxylates. The receptors also display significant cross-reactivity to the carboxylates, which enables the sensors to respond to a wide variety of carboxylate analytes. Generally speaking, it is the synergistic effect of the selective yet cross-reactive feature of the chemosensors that provides the good resolution (separation) of the clusters (carboxylates) in the PCA score plot.

In addition to the PCA, the multidimensional response pattern was further evaluated by linear discriminant analysis (LDA)[19] to explore the discriminatory power of the sensors array. LDA is a statistical approach widely used for classification using a cross-validation (leave-one-out) routine to assess the overall ability to correctly classify the observations. The LDA graphical output shows canonical score plots for the first three canonical factors (see Supporting Information, SI). Here, three factors describe 89.4% of the total information (variance) contained in the data set. This graphical representation shows clusters of similar data and demonstrates the quality and predictability of the output provided by the sensor array. The cross-validation routine shows 100% accuracy for the classification of all carboxylates (see SI).

Part of the motivation of this work was to establish the correlation between the structural features of sensors and the discriminatory power of the sensors array, an effort that could provide important information for developing an effective analytical device for carboxylate anions in physiological milieu. Toward this end, we determined which sensors contribute most to the discriminatory capacity. The screening of sensors was

dx.doi.org/10.1021/ja4015748 | J. Am. Chem. Soc. 2013, 135, 7705–7712

accomplished by excluding certain sensors utilizing a sequence of PCA followed by LDA.[12h] This way the sensors contributing most to the discriminatory power (as judged by PCA) remain in the array, whereas the less contributing sensors are excluded (Figure 6). An ideal array should comprise the lowest number of sensors that allow maintaining the 100% correct classification accuracy. Those should be the sensors contributing most to the individual principal component with statistical significance,[20] as estimated from the sensor contribution to the principal component. This contribution can be evaluated from the factor loadings which correlate to the cosine of the angle between the original variable and principal component axis.

Figure 6 shows the screening process for sensors. First, PCA is used to identify the three sensors (**S1**, **S5**, **S8**) with the highest contribution to statistically significant principal components (PC1, PC2, PC3). The selection of **S1**, **S5**, and **S8** makes sense from the supramolecular chemistry perspective as well because **S1** and **S2** display the highest affinity for acetate (as a model for aliphatic carboxylates, $K_a \approx 10^6$ M^{-1}, Table 1) while **S8** displays the overall highest selectivity (binds acetate but not benzoate, which is probably too large to fit well in the binding cavity of the tripodal receptor of **S8**). It is quite likely that the sensors with the highest affinity and selectivity would have the highest impact on the variance within the response data. We believe that it is the complementarity between **S5** and **S8** that increases the discriminatory capacity. We find it reassuring that our understanding of supramolecular chemistry principles and the pattern recognition methods arrive at the same conclusion. The LDA confirmed that the selection of the sensors **S1**, **S5**, and **S8** did not result in compromised classification accuracy.

Further exploring reveals that **S5** and **S8** are the most important contributors to discriminatory power of the array. An LDA cross-validation routine demonstrated that the two sensors still provide 100% correct classification, even though the response space is not as large as that with the eight sensors (Figure 6).

While from the array fabrication perspective it is convenient to decrease the number of the sensors in the array, from the view of need to record and work with a large amount of data from multiple channels one may be interested in learning about the lowest number of channels required for 100% correct classification of the 14 analytes (**D1**–**D14**). Toward this end, we performed a similar analysis as above aimed at evaluation of detection channels. We learned that when we use all eight sensors, we actually need only four channels to achieve 100% correct classification (for the LDA results, see the SI).

Finally, we also attempted the reduction of both the number of sensors in the array as well as the number of channels recorded. 100% correct classification was achieved with four sensors utilizing output in four channels. This corresponds to reduction of the original data set by 87% (only 13% of the original data set was used to recognize the 14 carboxylates **D1**–**D14**). This illustrates the excellent recognition capabilities of the sensors and suggests an approach one may use to reduce this method to practice.

The detection of carboxylates in biological fluids such as human urine is of clinical importance since the levels of drugs reflect the state of human health.[21] However, to detect carboxylates in urine is a challenging problem as urine is a highly competitive medium that contains high concentrations of electrolytes, such as chloride, phosphates, and carboxylates, as well as a large number of proteins. To accomplish the anion sensing in such a complex medium requires highly responsive sensing elements capable of distinguishing among a large number of similar analytes.

To obtain maximum discriminatory information, we also recorded the response from both the fluorimetric and colorimetric channels (combined 15 channels were recorded). Once again, multivariate statistical methods PCA and LDA were used to evaluate the response pattern. The PCA of the data set requires 20 dimensions (PCs) out of 120 to describe 95% of the discriminatory range (which corresponds to a mere 17% of all PCs). The PCA score plot (see the SI) shows clear clustering of the data with the first three PCs (representing 65.8% of variance). The high dispersion level of the data shown by the PCA score plot reflects the fact that the eight-member sensor array possesses high discriminatory capacity to the carboxylic drugs in urine. Similarly, the LDA canonical score plot (Figure 7) shows clear clustering of the data with the first

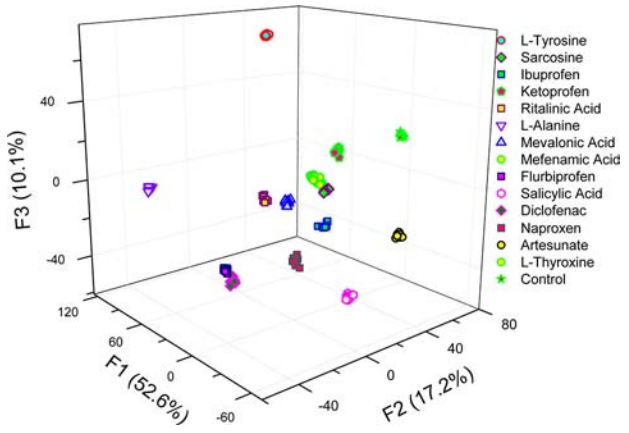

Figure 7. LDA canonical score plots for the response of **S1**–**S8** sensors array to fourteen carboxylates in urine. The first 3 factors were used in order to describe 80% of the total variance. The cross-validation routine shows 100% correct classification.

three factors describing 82.0% of the total information (variance) contained in the data set. LDA cross-validation routine shows 100% classification accuracy for the 14 carboxylates **D1**–**D14** in urine. This confirms that the **S1**–**S8** sensor array possesses very high discriminatory capacity even in a highly competitive milieu.

Due to the significance of NSAIDs, we decided to demonstrate the potential for quantitative sensing using the present method. Two analyses were performed: First, a quantitative analysis of ibuprofen and diclofenac was performed using the **PU**:**S3** film (Figure 8). Second, to illustrate the ability of the sensor array (**S1**–**S8**) to recognize multiple NSAID carboxylates, a semiquantitative analysis was applied to six carboxylates: Diclofenac, flurbiprofen, ibuprofen, salicylic acid, ketoprofen, and naproxen.

Figure 8 shows quantitative analyses of ibuprofen and diclofenac. The overall response isotherm displays saturation behavior and a linear portion at low analyte concentrations. The inset shows the linear response to ibuprofen and diclofenac in the concentration range of 0–4 ppm. Ibuprofen and diclofenac analysis suggests a limit of detection LOD $\approx$ 0.1 ppm. The fact that the **PU**:**S3** shows a reasonably low LOD attests to the potential applicability of this approach.

Encouraged by this result, analysis of six NSAID-related carboxylates was performed using the present sensors array

dx.doi.org/10.1021/ja4015748 | J. Am. Chem. Soc. 2013, 135, 7705–7712

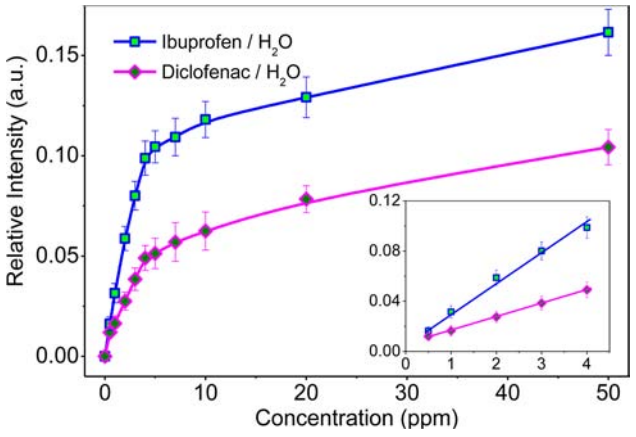

Figure 8. Concentration analyses of ibuprofen and diclofenac. The inset in the graph shows the linear region in the concentration range of 0−4 ppm. Analysis shows a limit of detection LOD ≈ 0.1 ppm.

(Figure 9). NSAIDs diclofenac, flurbiprofen, ibuprofen, salicylic acid, ketoprofen, and naproxen were tested in concentrations

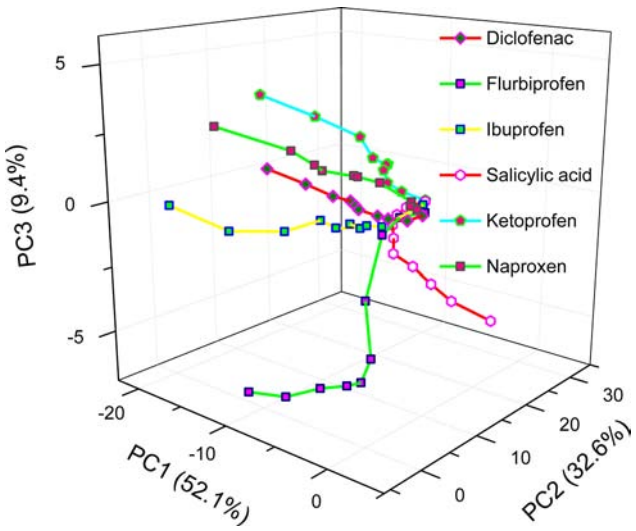

Figure 9. PCA score plots describe the response of the **S1**−**S8** array to six different NSAID carboxylates at a concentration range between 0.5 and 100 ppm. The response functions are derived from calculating the average of the scores for each concentration of a given drug. The limit of detection for six carboxylates is ∼0.1 ppm.

ranging from 0 to 100 ppm. First, PCA was carried out to reveal the clustering and the trends in the response data. The PCA was used to plot the concentration response function in the score plot space. Figure 9 shows response functions composed of the average scores for each concentration of a given carboxylate. From the concentration-dependent response functions, it can be seen that the sensor array was able to discriminate between six different carboxylates in a wide range concentration from 0.5 to 100 ppm, which covers the typical NSAIDs urinary concentration.[8b] It should be noted that the response functions are not the same as isotherms. The response functions are the result of dimensionality reduction to mere three dimensions. Thus, for each analyte, data from 150 variables are reduced to a response function, which is then projected into three-dimensional space (PC1 × PC2 × PC3).

As expected, all six response functions in Figure 9 originate from the same point (0 analyte concentration, control). This is also a reason why at low concentrations, the data points appear to be close. This is reasonable considering the isotherms shown in Figure 8. Importantly, however, all concentrations for all six NSAIDs are resolved (separated). It could be argued that one may not need an array sensor for six different analytes; indeed, six NSAIDs in a semiquantitative analysis was, in fact, a stress test rather than a realistic assignment. The significance of this result is in the proof of simultaneous quantitative sensing of anionic analytes utilizing an array-based approach at low concentration, which is a rare achievement.

■ CONCLUSIONS

This study demonstrates that the eight hydrogen-bonding based chemosensors embedded in hydrophilic polyurethane films can be used in sensor arrays for the detection of carboxylates in water or in urine. The seven sensors (**S1**−**S7**) utilize a common receptor, calix[4]pyrrole, attached to a chromophore via a conjugated moiety, thereby establishing an intramolecular partial charge transfer (IPCT) chromophore that yields a strong fluorescence and color change in the presence of anion. Another tripodal sensor (**S8**) was included in the array to increase the selectivity of the array and variance in the output data sets. Pattern recognition methods (PCA, LDA) were employed to evaluate the sensing performance of the array. The 14 carboxylates were detected in water with 100% classification accuracy. To demonstrate the practical utility, the 100% correct classification of carboxylates was performed in human urine. Finally, the simultaneous semi-quantitative analysis for six NSAIDs was performed in the wide range concentrations (0.5−100 ppm). It was demonstrated that the array responds to the presence of each NSAID analyte by an analyte-unique response which can be transformed in an isotherm-like function. Our preliminary results suggest that these dependences may be used as calibration curves for rigorous regression treatments. We believe that these results open up an avenue for development of future array sensors for detection of carboxylates in biological and health-related applications.

■ EXPERIMENTAL SECTION

Sensors **S1**,[12b] **S2**,[15f] and **S8**[12e] were previously synthesized. The synthesis and characterization of sensors **S3**, **S4**, **S5**, **S6**, and **S7** are described in the SI. The multiwell 15 × 8 (submicroliter) array chips were fabricated by ultrasonic drilling of microscope slides (well diameter: 1000 ± 10 μm, depth: 250 ± 10 μm). The sensor solutions (500 μM) were prepared by dissolving **S1**−**S8** in a polyurethane hydrogel Tecophilic THF solution (4 wt %). In a typical array, the sensor solution (200 nL) was spotted into the wells of the multiwell chip and dried to form a 5-μm thick polymer film in each well. The aqueous solutions of carboxylic drugs (200 nL, 500 μM or 1 mM), whose pH values adjusted at pH 8.5, were then added to each well containing the sensor.

The human urine used in the experiments displayed the following characteristics: pH 7.1, sodium ion (69 mEq/L), potassium (22.1 mEq/L), chloride (70 mEq/L), phosphate (34.8 mg/dL), creatinine (24.1 mg/dL), and μ-albumine (10 mg/L).

Images from the sensor array were recorded using a Kodak Image Station 440CF (for preliminary experiments) and a Kodak Image Station 4000MM PRO (for qualitative and semiquantitative experiments). The images recorded using the Image Station 4000MM PRO reflect both fluorescence (11 channels) and color intensity (four channels), respectively. In fluorescence detection, the combinations of channels (excitation (λ_{ex}) and emission (λ_{em}) filters) are as follows: λ_{ex}(430 nm)−λ_{em}(480 nm), λ_{ex}(430 nm)−λ_{em}(535 nm), λ_{ex}(430 nm)−λ_{em}(600 nm), λ_{ex}(470 nm)−λ_{em}(535 nm), λ_{ex}(470

dx.doi.org/10.1021/ja4015748 | J. Am. Chem. Soc. 2013, 135, 7705−7712

nm)−λ_{em}(600 nm), λ_{ex}(500 nm)−λ_{em}(535 nm), and λ_{ex}(500 nm)−λ_{em}(600 nm). No excitation filters were used when using broadband UV as the excitation light, and the combinations of channels are as follows: λ_{ex}(UV)−λ_{em}(440 nm), λ_{ex}(UV)−λ_{em}(535 nm), λ_{ex}(UV)−λ_{em}(480 nm), and λ_{ex}(UV)−λ_{em}(600 nm). In colorimetric detection using the 4000MM PRO, the filters for color-intensity measurement are 440, 480, 535, and 600 nm, respectively. After acquiring the images, the integrated (nonzero) gray pixel value (n) is calculated for each well in each channel. Images of the sensor chip were recorded before (b) and after (a) the addition of an analyte. The final responses (R) were evaluated as indicated in the following eq 1:

$$R = \sum_n \frac{a_n}{b_n} - 1 \quad (1)$$

■ ASSOCIATED CONTENT

Supporting Information

Synthesis and characterization of **S3**, **S4**, **S5**, **S6**, and **S7**, UV−vis and fluorescence spectra, and results of multivariate analysis. This material is available free of charge via the Internet at http://pubs.acs.org.

■ AUTHOR INFORMATION

Corresponding Author

pavel@bgsu.edu

Notes

The authors declare no competing financial interest.

■ ACKNOWLEDGMENTS

We gratefully acknowledge the financial support from the NSF (CHE-0750303 and EXP-LA 0731153 to P.A.) and BGSU (TIE Grant).

■ REFERENCES

(1) (a) Kroschwitz, J. I.; Seidel, A. *Kirk-Othmer Encyclopedia of Chemical Technology*, 5th ed.; Wiley-Interscience: Hoboken, N. J.: New York, 2007; Vol. *5*. (b) Ullmann, F.; Gerhartz, W.; Yamamoto, Y. S.; Campbell, T.; Pfefferkorn, R.; Rounsaville, J. F. *Ullmann's Encyclopedia of Industrial Chemistry*, 7th ed.; Wiley-VCH: Weinheim, 2011.

(2) (a) *Nonsteroidal Anti-Inflammatory Drugs: Mechanisms and Clinical Uses*, 2*nd ed.*; Lewis, A. J.; Furst, D. E., Eds. Marcel Dekker: New York, 1994; (b) Lemke, T. L.; Williams, D. A. *Nonsteroidal Anti-Inflammatory Drugs Foye's Principles of Medicinal Chemistry*, 6th ed.; Lippincott, Williams, & Wilkins: Philadelphia, 2008. (c) *Pharmacotherapy Handbook*, 8th ed.; Wells, B. G., DiPiro, J. T., Schwinghammer, T. L., DiPiro, C., Eds.; McGraw Hill: New York, 2012.

(3) (a) Corcoran, J.; Winter, M. J.; Tyler, C. R. *Crit. Rev. Toxicol.* **2010**, *40*, 287−304. (b) http://www.epa.gov/esd/bios/daughton/book-summary.htm.

(4) Li, Q.; Weina, P. *Pharmaceuticals* **2010**, *3*, 2322−2332.

(5) (a) Sreekumar, A.; Poisson, L. M.; Rajendiran, T. M.; Khan, A. P.; Cao, Q.; Yu, J.; Laxman, B.; Mehra, R.; Lonigro, R. J.; Li, Y.; Nyati, M. K.; Ahsan, A.; Kalyana-Sundaram, S.; Han, B.; Cao, X.; Byun, J.; Omenn, G. S.; Ghosh, D.; Pennathur, S.; Alexander, D. C.; Berger, A.; Shuster, J. R.; Wei, J. T.; Varambally, S.; Beecher, C.; Chinnaiyan, A. M. *Nature* **2009**, *457*, 910−914. (b) Wu, H.; Liu, T.; Ma, C.; Xue, R.; Deng, C.; Zeng, H.; Shen, X. *Anal. Bioanal. Chem.* **2011**, *401*, 635−646. (c) Solimana, L. C.; Hui, Y.; Hewavitharan, A. K.; Chen, D. D.Y. *J. Chromatogr. A* **2012**, *1267*, 162−169.

(6) Miziorko, H. M. *Arch. Biochem. Biophys.* **2011**, *505*, 131−143.

(7) Fernstrom, J. D.; Fernstrom, M. H. *J. Nutr.* **2007**, *137*, 1539S−1547S.

(8) (a) Hirai, T.; Matsumoto, S.; Kishi, I. *J. Chromatogr. B* **1997**, *692*, 375−388. (b) Aresta, A.; Palmisano, F.; Zambonin, C. G. *J. Pharm. Biomed. Anal.* **2005**, *39*, 643−647.

(9) Maurer, H. H.; Tauvel, F. X.; Kraemer, T. *J. Anal. Toxicol.* **2001**, *25*, 237−244.

(10) (a) Sessler, J. L.; Gale, P. A.; Cho, W.-S. *Anion Receptor Chemistry. Monographs in Supramolecular Chemistry*; Royal Society of Chemistry: Cambridge, 2006. (b) Bayly, S. R.; Beer, P. D. *Struct. Bonding (Berlin)* **2008**, *129*, 45−94. (c) Valeria, A.; Fabbrizzi, L.; Mosca, L. *Chem. Soc. Rev.* **2010**, *39*, 3889−3915. (d) Duke, R. M.; Veale, E. B.; Pfeffer, F. M.; Kruger, P. E.; Gunnlaugsson, T. *Chem. Soc. Rev.* **2010**, *39*, 3936−3953. (e) Li, A.-F.; Wang, J.-H.; Wang, F.; Jiang, Y.-B. *Chem. Soc. Rev.* **2010**, *39*, 3729−3745. (f) Wenzel, M.; Hiscock, J. R.; Gale, P. A. *Chem. Soc. Rev.* **2012**, *41*, 480−520. (g) Ngo, H. T.; Liu, X.; Jolliffe, K. A. *Chem. Soc. Rev.* **2012**, *41*, 4928−4965. (h) Pal, R.; Beeby, A.; Parker, D. *J. Pharm. Biomed. Anal.* **2011**, *56*, 352−358. (i) Butler, S. J.; Parker, D. *Chem. Soc. Rev.* **2013**, *42*, 1652−1666.

(11) (a) Gardner, J. W.; Bartlett, P. N. *Electronic Noses: Principles and Applications*; Oxford University Press: New York, 1999. (b) Rakow, N. A.; Suslick, K. S. *Nature* **2000**, *406*, 710−714. (c) Albert, K. J.; Lewis, N. S.; Schauer, C. L.; Sotzing, G. A.; Stitzel, S. E.; Vaid, T. P.; Walt, D. R. *Chem. Rev.* **2000**, *100*, 2595−2626. (d) Lavigne, J. J.; Anslyn, E. V. *Angew. Chem., Int. Ed.* **2001**, *40*, 3118−3130. (e) Anzenbacher, P., Jr.; Lubal, P.; Bucek, P.; Palacios, M. A.; Kozelkova, M. E. *Chem. Soc. Rev.* **2010**, *39*, 3954−3979. (f) Paolesse, R.; Monti, D.; Dini, F.; Di Natale, C. *Top. Curr. Chem.* **2011**, *300*, 139−174. (g) Stitzel, S. E.; Aernecke, M. J.; Walt, D. R. *Annu. Rev. Biomed. Eng.* **2011**, *13*, 1−25.

(12) (a) Nelson, T. L.; O'Sullivan, C.; Greene, N. T.; Maynor, M. S.; Lavigne, J. J. *J. Am. Chem. Soc.* **2006**, *128*, 5640−5641. (b) Palacios, M. A.; Nishiyabu, R.; Marquez, M.; Anzenbacher, P., Jr. *J. Am. Chem. Soc.* **2007**, *129*, 7538−7544. (c) Lavigne, J. J. *Nat. Mater.* **2007**, *6*, 548−549. (d) Palacios, M. A.; Wang, Z.; Montes, V. A.; Zyryanov, G. V.; Hausch, B. J.; Jursıkova, K.; Anzenbacher, P., Jr. *Chem. Commun.* **2007**, 3708−3710. (e) Zyryanov, G. V.; Palacios, M. A.; Anzenbacher, P., Jr. *Angew. Chem., Int. Ed.* **2007**, *46*, 7849−7852. (f) Wang, Z.; Palacios, M. A.; Zyryanov, G. V.; Anzenbacher, P., Jr. *Chem.−Eur. J.* **2008**, *14*, 8540−8546. (g) Wang, Z.; Palacios, M. A.; Anzenbacher, P., Jr. *Anal. Chem.* **2008**, *80*, 7451−7459. (h) Palacios, M. A.; Wang, Z.; Montes, V. A.; Zyryanov, G. V.; Anzenbacher, P., Jr. *J. Am. Chem. Soc.* **2008**, *130*, 10307−10314. (i) Shabbir, S. H.; Joyce, L. A.; da Cruz, G. M.; Lynch, V. M.; Sorey, S.; Anslyn, E. V. *J. Am. Chem. Soc.* **2009**, *131*, 13125−13131. (j) Suslick, B. A.; Feng, L.; Suslick, K. S. *Anal. Chem.* **2010**, *82*, 2067−2073. (k) Liu, Y.; Palacios, M. A.; Anzenbacher, P., Jr. *Chem. Commun.* **2010**, *46*, 1860−1862. (l) Feng, L.; Zhang, Y.; Wen, L. Y.; Chen, L.; Shen, Z.; Guan, Y. F. *Chem. −Eur. J.* **2011**, *17*, 1101−1104. (m) Davey, E. A.; Zucchero, A. J.; Trapp, O.; Bunz, U. H. F. *J. Am. Chem. Soc.* **2011**, *133*, 7716−7718. (n) Lin, H.; Jang, M.; Suslick, K. S. *J. Am. Chem. Soc.* **2011**, *133*, 16786−16789. (o) Zhang, X.; You, L.; Anslyn, E. V.; Qian, X. *Chem.−Eur. J.* **2012**, *18*, 1102−1110. (p) Anzenbacher, P., Jr.; Li, F.; Palacios, M. A. *Angew. Chem., Int. Ed.* **2012**, *51*, 2345−2348. (q) Lim, J.; Nam, D.; Miljanić, O. Š. *Chem. Sci.* **2012**, *3*, 559−563. (r) Minami, T.; Esipenko, N. A.; Zhang, B.; Kozelkova, M. E.; Isaacs, L.; Nishiyabu, R.; Kubo, Y.; Anzenbacher, P., Jr. *J. Am. Chem. Soc.* **2012**, *134*, 20021−20024.

(13) Kitamura, M.; Shabbir, S. H.; Anslyn, E. V. *J. Org. Chem.* **2009**, *74*, 4479−4489.

(14) Nishiyabu, R.; Anzenbacher, P., Jr. *J. Am. Chem. Soc.* **2005**, *127*, 8270−8271.

(15) For reviews, see: (a) Gale, P. A.; Anzenbacher, P., Jr.; Sessler, J. L. *Coord. Chem. Rev.* **2001**, *222*, 57−102. (b) Anzenbacher, P., Jr. *Top. Heterocycl. Chem.* **2010**, *24*, 205−235. (c) Anzenbacher, P., Jr. *Top. Heterocycl. Chem.* **2010**, *24*, 237−265. For examples, see: (d) Miyaji, H.; Sato, W.; Sessler, J. L. *Angew. Chem., Int. Ed.* **2000**, *39*, 1777−1780. (e) Nielsen, K. A.; Jeppesen, J. O.; Levillain, E.; Becher, J. *Angew. Chem., Int. Ed.* **2003**, *42*, 187−191. (f) Nishiyabu, R.; Anzenbacher, P., Jr. *Org. Lett.* **2006**, *8*, 359−362. (g) Sokkalingam, P.; Kim, D. S.; Hwang, H.; Sessler, J. L.; Lee, C.-H. *Chem. Sci.* **2012**, *3*, 1819−1824.

(16) (a) Gunnlaugsson, T.; Kruger, P. E.; Jensen, P.; Tierney, J.; Ali, H. D. P.; Hussey, G. M. *J. Org. Chem.* **2005**, *70*, 10875−10878. (b) Quinlan, E.; Matthews, S. E.; Gunnlaugsson, T. *J. Org. Chem.* **2007**, *72*, 7497−7503. (c) Duke, R. M.; Gunnlaugsson, T. *Tetrahedron Lett.* **2011**, *52*, 1503−1505.

(17) The choice of DMSO and MeCN was made because the binding behavior observed in these polar organic solvents is also observed in arrays when the sensor elements are embedded in polyurethane matrixes and the anions are administered as strictly aqueous solutions. See: Palacios, M. A.; Nishiyabu, R.; Marquez, M.; Anzenbacher, P., Jr. *J. Am. Chem. Soc.* **2007**, *129*, 7538−7544.
(18) The 120 dimensions = 15 channels × 8 sensors are composed of 88 dimensions (11 fluorescence channels × 8 sensors) and 32 dimensions (4 colorimetric channels × 8 sensors).
(19) (a) Jambu, M. *In Exploratory and Multivariate Data Analysis*; Academic Press: San Diego, 1991. (b) Beebe, K. R.; Pell, R. J.; Seasholtz, M. B. *In Chemometrics: A Practical Guide*; Wiley: New York, 1998. (c) Otto, M. *Chemometrics, Statistics and Computer Application in Analytical Chemistry*; Wiley-VCH: Chichester. 1999.
(20) (a) Carey, W.; Beebe, K.; Kowalski, B. *Anal. Chem.* **1986**, *58*, 149−153. (b) Avila, F.; Myers, D.; Palmer, C. *J. Chemometrics* **1991**, *5*, 455−465. (c) Green, E.; Olah, M. J.; Abramova, T.; Williams, L. R.; Stefanovic, D.; Worgall, T.; Stojanovic, M. N. *J. Am. Chem. Soc.* **2006**, *128*, 15278−15282.
(21) (a) Turley, S. M. *Understanding Pharmacology for Health Professionals*, 3rd ed.; Prentice Hall: New York, 2002; (b) Cohen, B. J. *Medical Terminology: An Illustrated Guide*, 4th ed.; Lippincott, Williams, & Wilkins: Philadelphia, 2003.